Thermo-mechanical, antimicrobial and biocompatible properties of PVC blends based on imidazolium ionic liquids

Daniela Zampino[a,*], Monique Mancuso[b], Renata Zaccone[c], Tiziana Ferreri[d], Assunta Borzacchiello[e], Stefania Zeppetelli[e], Sandro Dattilo[a], Martina Ussia[f], Loredana Ferreri[a], Domenico C. Carbone[a], Giuseppe Recca[a], Concetto Puglisi [a]

[a]*Institute of Polymers, Composites and Biomaterials (IPCB)-CNR, Section of Catania, Via Paolo Gaifami, 18, 95126 Catania, Italy. E-mail: danielaclotilde.zampino@cnr.it*
[b]*Institute for Biological Resources and Marine Biotechnology (IRBIM)-CNR, Section of Messina, Spianata San Raineri 86,98122 Messina, Italy.*
[c]*Institute of Polar Science (IPS)-CNR, Section of Messina, Spianata San Raineri 86,98122 Messina, Italy.*
[d]*Institute of Biomolecular Chemistry (ICB)-CNR, Section of Catania, via Paolo Gaifami 18, Catania, 95126, Italy*
[e]*Institute of Polymers, Composites and Biomaterials (IPCB)-CNR, Viale Kennedy n.54, Pad.20, 80125 Napoli, Italy*
[f] *Institute for Microelectronics and Microsystems (IMM)-CNR, Via Santa Sofia 64, 95123 Catania, Italy*

Abstract

The aim of this study was the development of antimicrobial polyvinylchloride (PVC) blends loaded with 0.1-10% (w/w) of the ILs 1-hexadecyl-3-methylimidazolium 1,3-dimethyl 5-sulfoisophthalate (HdmimDMSIP) and 1-octyloximethyl-3-methylimidazolium hexafluorophosphate (OOMmimPF$_6$). The synthetized ILs were characterized by ^{1}HNMR, MALDI-TOF, DSC and TGA. PVC/ILs films were obtained by *solvent casting*.Thermal and mechanical properties (tensile stress TS and elongation at break EB), morphology by SEM, surface wettability, antimicrobial activity, cytotoxicity and ILs release in sterile water from PVC/ILs film blends were determined. Results demonstrated that the presence of both ILs in PVC formulation slightly affected thermal and mechanical properties of blends. The loading of both ILs into PVC matrix made PVC/ILs films hydrophilic, especially at the highest concentration of HdmimDMSIP. The PVC/ILs blends displayed antibacterial activity up to

ILs lowest concentrations (0.1-0.5 %). The inhibition of *Escherichia coli* growth was lower than that showed towards *Staphylococcus epidermidis*. The addition of 10% ILs concentration resulted excessive as demonstrated by accumulation of ILs on film surfaces (SEM) and ILs high release from PVC/ILs blends during the first day of water immersion. Biocompatibility studies highlighted that the addition of low amounts of both ILs into PVC matrix is not cytotoxic for mouse fibroblast cells (L929), supporting their potential use for biomedical porposes.

1. Introduction

The increasing number of infections due to antibiotic drugs resistance represents a constant challenge to human safety, in particular in hospitalized patients. Consequently, the availability of antimicrobial polymer materials is undoubtedly important for health care applications. The possibility of incorporating antimicrobial agents into polymer matrix without affecting polymer properties and performance is certainly remarkable from an industrial point of view. Particular attention, however, should be given to the choice of the antimicrobial compounds to be used. In fact, in addition to possessing the specific bactericidal, bacteriostatic or antibiotic function, they must also have physical and chemical characteristics that allow them to be easily incorporated into polymeric matrices, avoiding complex synthesis procedures. To impart antimicrobial properties to materials, silver salts, silver zeolites and nanoparticles, peptides, cationic compounds (or polymers) have been intensively studied [1,2]. Moreover, a large number of antimicrobial ILs have been synthetized as suitable alternatives to widely used biocides and antiseptics, as benzalkonium chloride (BAC) and cetylpyridinium chloride (CPC) [3,4].

Ionic liquids (ILs) are a very interesting class of low temperature molten salts containing organic cations, mainly constituted by head groups with attached one or more aliphatic alkyl chain substituents, and organic or inorganic anions. These salts have attracted research attention for their interesting properties, such as thermal stability, low or no flammability, negligible vapor pressure, solvation ability, biocompatibility or low toxicity [5,6]. The large number of cation/anion combinations and the possibility to structurally adjust this family of compounds may provide an advance to design optimized ILs, which can be utilized for specific applications. ILs have been applied in synthetic chemistry to improve reaction rates and selectivity, as safer alternatives for VOCs (Volatile Organic Compound) in "Green Chemistry", and as solvents in several catalytic organic reactions and polymerization processes [7-11]. Moreover, they have been employed in electrochemistry, electrochemical sensors preparation, separation/extraction techniques, metal extraction, gas separation, nanoparticle formation, IL-based polymer electrolytes, dispersants [12-

17]. In polymer science and biological applications they have been used as surfactants, plasticizers, polymer gels, oxygen transport membranes, porous polymers, APIs (Active Pharmaceutical Ingredients), biosensors, scaffold for biomimetic applications, antiarrhythmic, antimicrobial, antimetastic and anti-inflammatory agents [7,12,18,19].

The strong antimicrobial activity of imidazolium ILs, comparable to that of commercial compounds such as Triclosan [20], is mainly due to the alkyl chain length in the cation. Indeed, it has been reported [3,4,21,22] that the easy interaction between ILs with long alkyl substituents (12-16 methylene groups) and bacteria cell membrane damages membrane integrity causing cell death.

The antimicrobial activity against bacteria growth of neat ILs has been mainly evaluated by the determination of the minimum inhibition concentration (MIC) and the minimum bactericidal concentration (MBC). Moreover, ILs have been introduced into different polymeric materials (PMMA, PVC, PBT, PC, PET, PLA, Pebax®Rnew, etc.) as plasticizer [23-25], antimicrobial agents [20, 26-31], for the production of IL calcium phosphate-based bionanocomposites [32]. Recently, the synthesis of cationic poly(ionic liquids) (PILs), incorporating ILs into polymer chains, led to interesting polymeric materials for multiple applications, in particular for the development of new antimicrobial systems [33].

It was previously reported [20,27] that polyesters (PBT, PET) functionalized with imidazolium ILs displayed marked antibacterial activity at low ILs content (2%). Although incorporation of ILs into polymer matrix by functionalization allows to obtain antimicrobial composites more stable than blending, for an easy industrial production, the addition of ILs into polymer matrix by blending is more simple, low-cost and less time-consuming.

The polyvinyl chloride (PVC) is a versatile material widely used in different industrial sectors (building and construction, pipelines, waterproof clothing, medical items) for its low cost, compatibility with different additives, easy processability. In medical and healthcare fields, PVC is employed for the production of catheters, tubing for blood transfusions, bags for body fluids collection, gloves, oxygen masks, overshoes, etc. Due to its widespread use, in this study we prepared antimicrobial PVC blends containing different percentages of the 1-hexadecyl-3-methylimidazolium 1,3-dimethyl 5-sulfoisophthalate (HdmimDMSIP) and 1-octyloximethyl-3-methylimidazolium hexafluorophosphate (OOMmimPF$_6$) ILs. Taking into account literature data, we chose these two ILs, differing for the alkyl chain structure and length of the imidazolium cations and the hydrophobicity/hydrophilicity properties of the anions, to evaluate the influence of different cation and anion structures on antibacterial activity.

Considering phthalates exposure and environmental and human health concerns, we used a phthalate-free PVC formulation, plasticized with trioctyl trimellitate (TOTM). PVC/ILs films were obtained by

solvent casting, using tetrahydrofuran (THF) as solvent. Thermal and mechanical properties together with antimicrobial activity, biocompatibility and cytotoxicity of the film blends were analyzed. Moreover, an accurate and easy method for the simultaneous quantification of cations and anions released in water from PVC/ILs blends was used. Finally, to determine surface distribution of ILs and wettability of the antimicrobial film blends, SEM and contact angle analyses were carried out.

2. Materials and methods

2.1. Materials

PVC plasticized with tris (2-ethylhexyl) trimellitate (TOTM), having hardness (shore A) of 87.5, K-value of 65.0, specific gravity of 1.242, was provided by Consorzio Proplast (Alessandria, ITALY), whereas 1,3-dimethyl 5-sulfoisophthalate sodium salt (NaDMSIP), 1-methylimidazole, 1-bromohexadecane, chloromethyl octyl ether, sodium hexafluorophosphate, dichloromethane (DCM), ethyl acetate, tetrahydrofuran (THF), hexane, dimethyl sulfoxide-d_6 (DMSO-d_6), trans-2-[3-(4-tert-butylphenyl)-2-methyl-2-propenylidene]malononitrile, acetonitrile, sodium p-toluenesulfonate and 1-decyl-3-methylimidazolium chloride were purchased by Sigma Aldrich (Italy). All the chemicals were high purity products and were used as received.

2.2. Synthesis of Ionic Liquids

The synthesis of the selected ILs, carried out with slight modifications according to Colonna et al. [20] and Pernak et al. [34], respectively, has been previously reported by Clarizia et al. [31].

2.2.1. Synthesis of 1-hexadecyl-3-methylimidazolium dimethyl-5-sulfoisophthalate (HdmimDMSIP)

6.4 mL (20 mmol) of 1-bromohexadecane and a solution of 1-methylimidazole (1.56 mL, 20 mmol) in ethyl acetate (4 mL) were reacted in a controlled atmosphere (nitrogen) for 24 h at 65 °C under stirring. After cooling down to room temperature, the 1-hexadecyl-3-methylimidazolium bromide (HdmimBr) obtained was filtered and washed with ethyl acetate to remove unreacted initial compounds. Finally, the white solid was dried under vacuum at 40 °C for 24 h (yield 95.6%).

^{1}H NMR (400 MHz, DMSO-d_6, δ ppm): 0.84 (t, 3H, CH$_3$-C$_{15}$), 1.23 (m, 26H, CH$_2$), 1.77 (m, 2H, CH$_2$-CH$_2$-N), 3.85 (s, 3H, CH$_3$-N), 4.15 (t, 2H, CH$_2$-N), 7.72 (s, 1H, CH in imidazolium ring), 7.78 (s, 1H, CH in imidazolium ring), 9.15 (s, 1H, N-CH-N in imidazolium ring).

A solution of HdmimBr (20 mmol, 7.77 g) in 40 mL of dichloromethane (DCM) and a water solution (130 mL) of 1,3-dimethyl 5-sulfoisophthalate sodium salt NaDMSIP (20.9 mmol, 6.03 g) were placed in a separating funnel and vigorously shaken until no precipitate was present in the resulting two-phase mixture (30-45 min). After separation of the two phases, the organic layer was recovered, dried over magnesium sulfate and filtrated. The residual solvent was removed by rotavapor. The obtained product (HdmimDMSIP) was washed with ethyl acetate and dried at 40 °C in a vacuum stove for 24 h (yield 92.0%). The complete exchange of the bromide counter-ion was verified analyzing aliquots of the organic layer by the silver nitrate test. If the exchange was not complete, a new water solution containing the NaDMSIP salt was reacted with the organic layer to complete the anions exchange. The final product was a white powder.

^{1}H NMR (400 MHz, DMSO-d_6, δ ppm): Signals of imidazolium ring and alkyl chain: 0.84 (t, 3H, CH_3-C_{15} chain), 1.22 (m, 26 H, CH_2), 1.75 (m, 2H, CH_2-CH_2-N), 3.83 (s, 3H, CH_3-N), 4.14 (t, 2H, CH_2-N), 7.69 (s, 1H, CH in imidazolium ring), 7.75 (s, 1H, CH in imidazolium ring), 9.10 (s, 1H, N-CH-N in imidazolium ring). Signals of benzene ring: 3.90 (s, 6H, CH_3-O), 8.37 (d, 2H, CH, ortho position with respect to SO_3^- substituents), 8.42 (d, 1H, CH, para position with respect to SO_3^- substituents).

2.2.2. Synthesis of 1-octyloxymethyl-3-methylimidazolium hexafluorophosphate (OOMmimPF$_6$)

A mixture containing 3.86 mL (0.02 mol) of chloromethyl octyl ether and 1-methylimidazole (1.585 mL, 0.02 mol) was stirred under nitrogen, at room temperature, for 30 minutes. The obtained 1-octyloxymethyl-3-methylimidazolium chloride OOMmimCl was purified by several washings with hot hexane (at 50 °C) and filtrated. Then a reaction of ions exchange between sodium hexafluorophosphate (NaPF$_6$) (10 mL water solution, 0.02 mol) and OOMmimCl (10 mL water solution, 0.02 mol) was carried out keeping the mixture under stirring at 50 °C for 2 h. The final product was cooled down at room temperature and the organic fraction was separated by centrifugation at 3000 rpm for 5 min (yield 95%).

^{1}H NMR (400 MHz, DMSO-d_6, δ, ppm): 0.85 (t, 3H, CH_3–C_7 chain), 1.23 (m, 10 H, CH_2), 1.48 (m, 2H, CH_2-CH_2-O), 3.47 (s, 2H, CH_2-O), 3.88 (t, 3H, CH_3-N), 5.54 (s, 2H, O-CH_2-N), 7.76 (s, 1H, CH in imidazolium ring), 7.85 (s, 1H, CH in imidazolium ring), 9.28 (s, 1H, N-CH-N in imidazolium ring).

2.3. PVC/ILs films preparation

Before films realization, PVC pellets and ILs powder were dried under vacuum at 50 °C for 24 h. PVC/ILs film blends were prepared by *solvent casting* from THF solutions of 10 g/100 mL polymer concentration and ILs content of 0.1, 0.5, 1, 5 and 10% by weight percent of PVC. The PVC/ILs solutions were vigorously stirred at 40 °C for 4-5 h. Fixed aliquots of the mixtures were cast on glass plates, followed by solvent evaporation overnight at room temperature to produce films of 100-120 μm thick.

2.4. Characterization

2.4.1. NMR Spectroscopy

^{1}H NMR spectra of ILs samples were acquired at 20 °C on a Bruker Avance^{TM} 400 spectrometer, using the TOPSPIN 2.1 acquisition software. Samples were solubilized in dimethyl sulfoxide (DMSO-d$_6$) at a concentration of 10 mg/ml.

2.4.2. Matrix Assisted Laser Desorption Time of Flight Mass Spectrometry (MALDI TOF MS) Analysis

For MALDI TOF analysis a 4800 MALDI TOF/TOF™ Analyzer (Applied Biosystem, Framingham, MA, USA), equipped with a Nd:YAG laser (wavelength of 355 nm) of < 500 ps pulse and 200 Hz repetition rate and working in positive-ion mode was used. MALDI mass spectra were recorded in reflector mode. For masses in the range m/z 200-1000 Da, the mass resolution and accuracy of the MALDI spectra were about 10.000 (full width at half maximum, FWHM) and 1-10 ppm, respectively. Samples preparation was performed by dissolving in THF both ILs (10 mg/mL) and the matrix trans-2- [3- (4-tert-Butylphenyl) -2-methyl-2-propenyldene] malononitrile (0.1 mmol). Appropriate volumes of ILs and matrix solutions were mixed to obtain 1:1, 1:2 and 2:1 ratios (sample/matrix v/v). 1 μL of each sample was deposited onto the MALDI sample holder and dried at room temperature to allow matrix crystallization. The structural identification of MALDI peaks in Table 1 was mainly made on the basis of empirical formulas, taking into account the value of the isotopic mass distribution.

2.4.3. Calorimetric measurements

A differential scanning calorimeter (DSC, TA Instruments Q100), equipped with a liquid sub ambient

accessory and calibrated with high purity standards (indium and cyclohexane) was used for calorimetric measurements. Nitrogen was used as purge gas. The rate of heating and cooling cycles was 15 °C/min from -90 to 200 °C. Sample weight was in the range 4-6 mg.

2.4.4. Thermogravimetric analyses (TGA)

The thermogravimetric analyses were performed using a thermogravimetric apparatus (TGA, TA Instruments Q500) under a nitrogen atmosphere at 10 °C/min heating rate, from 50 °C to 600 °C. Sample weights were in the range 4-6 mg. The weight loss percent and its derivate (DTG) were recorded as a function of temperature.

2.4.5. Mechanical properties

The mechanical properties of compounds were measured by a tensile test machine (Zwick/Roell Z050) according to microtensile ASTM D1708. In particular, tensile strength (σ) and elongation at break percentage (ε) were analyzed. At least five replicates from each compound were realized by a microtensile cutter die and tested.

2.4.6. Scanning Electron Microscopy (SEM)

The surface morphology of PVC and PVC loaded with 10% of HdmimDMSIP and OOMmimPF$_6$ was performed by using a Gemini Field Emission SEM (FE-SEM) Carl Zeiss SUPRA 25. Prior SEM characterization, samples were prepared depositing 5 nm thick of gold by sputtering method.

2.4.7. Contact Angle (CA)

Wettability tests were carried out at 25°C by using a DATAPHYSICS-OCA 15 PRO apparatus and water as liquid. In detail, a drop (4 µl) of deionized water was formed on sample surface, regulating its volume by the software of the optical tensiometer. After drop stabilization (~ 10 seconds), three measurements on different areas, from the center and both lateral parts of the same sample, were performed. CA results are average values (± 2° standard deviation) of the three different measurements made on each sample.

2.5. ILs release

For ILs release determination round specimens (4 cm^2 surface) of PVC blend films loaded with 10% and 1% of ILs were used. Samples (at least three replicate specimens) were immersed on glass tubes containing sterile water (5 mL), incubated at 37 °C for 15 days and removed after 1, 5, 10 and 15 days.

To determine the daily release of ILs from PVC blends, samples were immersed in distilled water at 37 °C for 1 day, then they were removed and, after washing with distilled water, incubated again in fresh water medium for another 24 h and removed once again, repeating this procedure for 10 days on the same sample. The water media samples from the two methods described above were freeze-dried. The residue was recovered with 1.5 ml of acetonitrile and filtered. The attained samples were diluted before analysis and used for the determination of ILs released during the fixed time period (1, 5, 10, 15 days) and for the ILs daily release.

The concentration of ILs released in the water medium was determined by an UHPLC system, equipped with autosampler, coupled to an Orbitrap MS single-stage (Exactive ™, Thermo Fisher Scientific, Bremen, Germany) and operating with heated electrospray interface (HESI-II, Thermo Fisher Scientific).

The determination of ILs cation and anion concentration was performed by the direct infusion method. The UHPLC autosampler was used for the direct introduction of sample (1 μL) into the mass spectrometer. A mobile phase consisting in ACN/H$_2$O 50/50 v/v was used by isocratic elution at a flow rate of 0.1 mL/min.

The concentration of ILs cations and anions released in distilled water after the incubation time periods was determined through the construction of calibration curves (ILs concentration from 0.25 to 2.0 μg/mL) of the Hdmim and the OOMmim cations and the DMSIP anion, using the internal standard method, and for the PF$_6$ anion, using the external standard method. The internal standards used for the construction of the calibration curves, both at a concentration of 1 ppm, were 1-decyl-3-methylimidazolium chloride for the Hdmim and OOMmim cations and p-toluene sulfonate for the DMSIP anion.

2.6. Antibacterial screening

2.6.1. Bacterial strains growth

The two strains *Escherichia coli* and *Staphylococcus epidermidis* used in this study were isolated from the human urinary tract and kindly provided by the Department of Biomedical and Dental

Sciences and Morphofunctional Imaging, University of Messina (Italy).

Before antimicrobial analyses, the two strains were seeded on Tryptic Soy Agar medium (TSA, Oxoid) and incubated at 37 °C for 24 h. After collection and suspension in sterile saline solutions, strains concentrations were adjusted to 10^6 cell/mL by the McFarland tube.

2.6.2. Antibacterial tests

The Minimal Inhibitory Concentration (MIC) *vs* both *E. coli* and *S. epidermidis* strains of neat ILs was performed by the broth dilution method [35]. Initial sterile saline water solutions containing the ILs at 10 mg/ml (1% w/v concentration) were performed at 80-100°C under stirring for 5 min, immediately followed by serial dilutions, from 1 mg/ml to 1 µg/ml. The dissolution of OOMmimPF$_6$ was improved by adding to the initial water solution DMSO at a 10% concentration (v/v). In each tube, a bacterial suspension at the concentration of 10^6 cell/mL of *E. coli* or *S. epidermidis* was added. Samples were incubated at 37 °C and naked eye read after 24 h. The Minimal Bactericidal Concentration (MBC) of the tested antimicrobial agents was determined by subculturing in agar plate the lower broth dilution of MIC test, showing no turbidity and inducing a bacteria reduction ≥99.9%. The antibacterial activity of PVC/ILs blends was performed by the agar diffusion method (modified Kirby–Bauer). Before microbiological analyses, samples of neat PVC and PVC containing 0.1-10% (w/w) of ILs were sterilized by a UV lamp (wavelength 280–240 nm) through two steps of 3 min, according to Zampino et al. [1]. Samples were placed on the surface of TSA plates, seeded with *E. coli* or *S. epidermidis*, both strains at an initial concentration of 10^6 colony forming units (CFU)/mL), and incubated at 37 °C for 24 h. The antimicrobial activity of the PVC/ILs film compounds was determined by measuring the width in millimeters of the inhibition zone surrounding the polymeric samples.

2.7. Biological properties

2.7.1. Cell Culture

The L929 cells originating from Mouse C3H/An connective tissue were obtained from the European Collection of cell cultures (Sigma -Aldrich). L-929 cells for the performed experiments were used at a passage 15–23. The cells were grown in T-75 cell culture flask, in cell culture medium Dulbecco's Modified Eagle's Medium supplemented with 10% fetal bovine serum, 2mM glutamine and

antibiotics (penicillin G sodium 100 U/mL, streptomycin 100 g/mL) at 37 °C and 5% CO_2. When confluent growth was reached, the cells were detached with 0.25% trypsin-EDTA solution, washed twice with PBS. Cell suspension was centrifuged for 5 min at 1200 rpm. The supernatant was separated and cells were resuspended in fresh culture medium. Viable cells were counted using the TC20 automated Cell Counter.

2.7.2. Cytotoxicity assay

The biocompatibiity/cytotoxicity of neat ILs was evaluated by the Alamar blueTM assay against L929 cell lines seeded, in triplicate, in a 48-well plate at a concentration of 2×10^4 cell/well. Each plate contained negative (supplemented DMEM) and positive (phenol 6.4 g/l) controls, and the ILs series (three replicates each) at five concentrations (1, 5, 10, 25, 50 µg/mL).

After 24 h of incubation with HdmimDMSIP and OOMmimPF$_6$, the cell viability was checked by Alamar blueTM assay. An aliquot of 200 µL of Alamar BlueTM diluted 1:10 in phenol red-free medium was added to each well and incubated for a further 3 h at 37 °C, 5% CO_2. Later, 100 µL of this solution was transferred into a 96-well plate for colorimetric analysis. Wells without any cells were used to correct any background interference from the redox indicator. The absorbance was immediately measured using a spectrophotometer plate reader (Multilabel Counter, 1420 Victor, Perkin Elmer) at 570 nm and 600 nm wavelengths. AB is an indicator dye that incorporates an oxidation-reduction indicator that changes color in response to the chemical reduction in growth medium, resulting from cell viability. The cell viability percentage was evaluated according to the manufacturer's protocol. Data are expressed as the percentage difference in reduction (% AB reduction) between treated and control cells (~100% AB reduction) in viability assay:

$$\% \text{ AB Reduction} = \frac{(O_2 \times A_1) - (O_1 \times A_2)}{(O_2 \times P_1) - (O_1 \times P_2)} \times 100$$

where O_1 is the molar extinction coefficient (E) of oxidized AB at 570 nm; O_2 is the E of oxidized AB at 600 nm; A_1 is the absorbance of test wells at 570 nm; A_2 is the absorbance of test wells at 600 nm; P_1 is the absorbance of positive growth control well at 570 nm; P_2 is the absorbance of positive growth control well at 600 nm.

The *in vitro* cytotoxicity of PVC/ILs blends was evaluated by the elution test method (ISO 10993-5) [36]. PVC samples containing different amounts of ILs, previously sterilized by a UV-lamp 280-240 nm, were immersed in complete culture medium (2 mL/sample). The medium was incubated at 37 °C, occasionally shaken and at predetermined times (1, 5, 10, 15 days) a fixed quantity of medium (eluate) was taken and replaced with fresh medium. After incubation, the eluate was recovered and tested with the cell cultures without filtering, diluting or buffering, by putting it in contact with the L929 cells.

In particular, a concentration of $2*10^4$ cell/well was seeded directly in flat bottomed 48-well and after sub confluency. Negative (supplemented DMEM) and positive (phenol 6.4 g/l) controls were used. After 24 h of incubation, cell viability was assessed with the Alamar Blue (AB) assay. AB was added to the samples (10% v/v of medium) and incubated at 37 °C for 3 h. The measurements of the samples absorbance and the determination of % AB reduction were performed as detailed above.

3. Results and discussion

3.1. Synthesis and characterization of ILs and preparation of PVC/ILs blends

Both ILs were synthetized by a two steps method. The first step of synthesis has involved the alkylation and quaternization of 1-methylimidazole, yielding 1-hexadecyl-3-methylimidazolium bromide or 1-octyloxymethyl-3-methylimidazolium chloride, respectively. The second step was a reaction of metathesis between the bromide/chloride synthetized with the appointed inorganic salts in water solutions.

The characterization of the synthetized ILs was performed by ^{1}H NMR (Figs. SI 1, SI 3) and MALDI TOF (Table SI 1, Figs. SI 2, SI 4). The attributions of the peaks in the ^{1}H NMR spectra corresponding to the structures described in the experimental section show that the imidazole ring functionalization of the ILs took place. The ^{1}H NMR analysis of the synthetized products confirmed that the chemical shifts of the protons in the imidazole ring are anion-dependent, increasing with the increase of anion basicity, and consequently H-bonding capability (δ ppm = 7.69, 7.75 and 9.10 for HdmimDMSIP, 7.72, 7.78, and 9.15 for HdmimBr, as previously observed in other ILs [34, 37].

The analysis of the MALDI TOF spectra (Table SI 1; Figs. SI 2, SI 4) corroborated the successful outcome of the syntheses.

Both ILs synthetized were kept in a vacuum dryer during storage. The PVC/ILs films, prepared by *solvent casting*, had similar thickness (100-120 μm). The PVC/HdmimDMSIP films were colorless, whereas the PVC/OOMmimPF$_6$ ones were yellowish, mostly at high concentration of IL (Fig. SI 5). Both type of films were soft and transparent, indicating good ILs dispersion into the polymer matrix.

3.2. Thermal analysis

Generally, during molding and processing technologies for industrial production of end products may occur degradation processes that could affect the performance of materials. The thermal properties evaluation of neat ILs and PVC/ILs blends was performed by DSC and TGA. The characterization

by DSC and TGA of the neat ILs was previously reported in Clarizia et al. [31].

3.2.1. DSC measurements

Measurements of crystallization (T_c), glass-transition (T_g) and melting (T_m) temperatures were determined by DSC cooling and heating scans at 15 °C/min from -90 °C to 200 °C. The T_g and T_m temperatures, registered during the heating cycle, are the midpoint of a change from the amorphous glass state to a liquid state and the onset of an endothermic peak, respectively. The T_c and the cold crystallization (T_{cc}) temperatures are exothermic peaks during the cooling and the heating cycles, respectively. The analysis of HdmimDMSIP DSC curves (Fig. SI 6) revealed transitions at 49 °C and at -4 °C associated with T_m and T_c peaks, respectively, whereas the T_g was not detected at the experimental conditions adopted. The second heating scan evidenced a polymorphic behavior of this IL, as previously observed for other ILs [38,39].
DSC analysis of OOMmimPF$_6$ (Fig. SI 7) showed T_m and T_c values of 52 °C and 7 °C, respectively.

To avoid environmental and human health concerns from phthalates exposure, the neat PVC used for all experiments was plasticized with TOTM. DSC analysis of neat PVC revealed a glass transition temperature (T_g) of 64 °C during the first heating cycle, not detected during the second one (Fig. 1). This behavior was also observed from the thermal analysis of PVC blends loaded with the different concentrations of both ILs (Figs. SI 8, SI 9), showing no estimable T_g during the second heating cycle. Since in this study we used plasticized PVC, the eventual plasticizing effect of the ILs, loaded in the PVC matrix in concentrations up to 10%, becomes secondary because it is obscured by the primary one of the TOTM. To verify the possible plasticizing effect of ILs, additional analyses were performed by using un-plasticized PVC powder (Sigma Aldrich, Italy) and ILs at concentrations of 10-30% (w/w). Results showed a 6°C and 20°C decrease of T_g from un-plasticized PVC film (about 71°C) to PVC/10%ILs and PVC/30%ILs blends, respectively (Fig. 2).
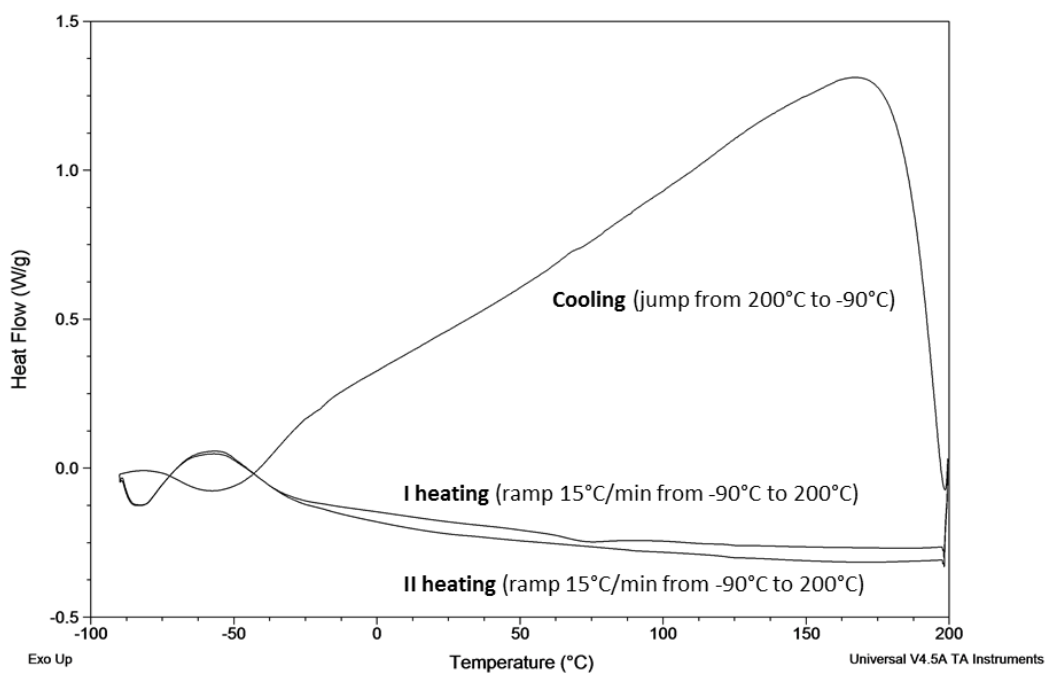
Fig. 1 DSC curves of neat PVC TOTM.

The T_g (50°C) is visible for PVC/30% HdmimDMSIP blend, whereas it is not detectable for PVC/30% OOMmimPF$_6$, probably because it occurs in the temperature range of 42-56°C, which corresponds to the endothermic transition (T_m) of OOMmimPF$_6$ observed at 49.7°C.
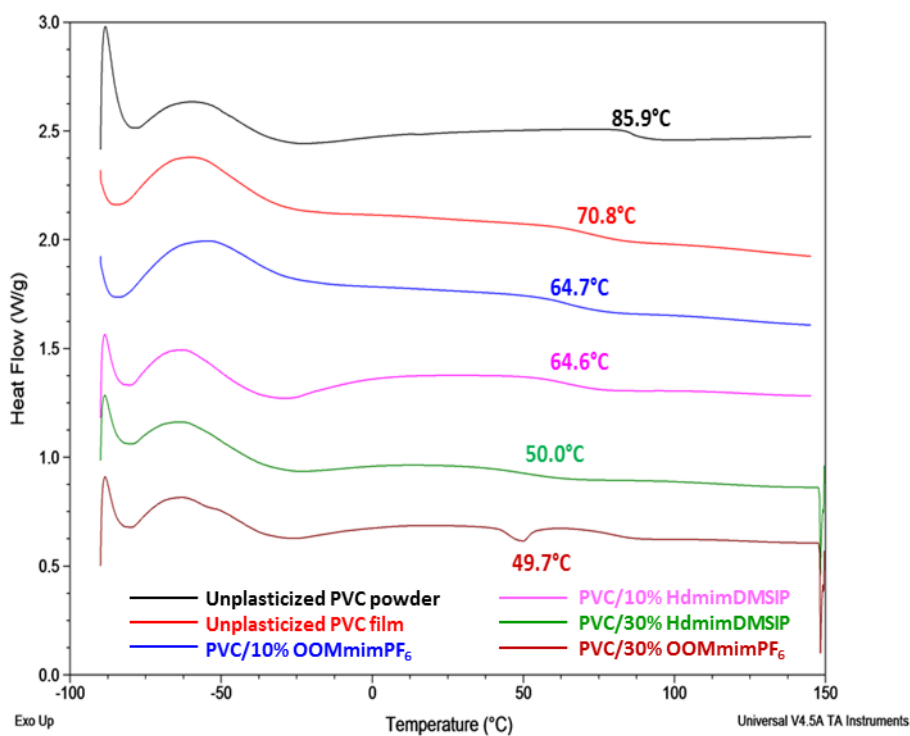

Fig. 2 DSC curves from II heating cycle of un-plasticized PVC (powder and film) and PVC blend films loaded with ILs at 10-30% (w/w) concentrations. Scans are shifted for clarity

The addition of both long side-chain ILs into PVC matrix increased the plasticization of PVC/ILs blends, probably by reduction of molecule forces and steric hindrance and increase of free volume [25]. Our results are in agreement with previous reports. Rahaman and Brazel [24] stated that all imidazolium-based ILs they studied successfully lowered the T_g of PVC. Hou and Wang [25] reported that ionic liquids decreased T_g of PVC samples from 58 °C for un-plasticized PVC to 38 °C and 25 °C for butyl methylimidazolium PF_6 and hexyl methylimidazolium PF_6 plasticized PVC film samples, respectively. Scott et al. [23], studying the use of ILs as low-volatility plasticizers for PMMA, detailed that the incorporation into PMMA matrix of ILs up to 50 vol.% lowered below room temperature T_g of PMMA, founding a remarkably linear relationship between T_g and plasticizer content.

3.2.2. Thermal stability measurements

Preliminary thermogravimetric analyses from 30 °C to 800 °C showed a thermal behavior similar to that reported in Tables 1, 2. The only difference observed was a slight (up to 1 wt%) decrease of residues, thus for the following analyses we used the 40-600 °C temperature range of degradation. We used TGA short-term (ramped) experiments as they provide reliable information on thermal stability of various ILs and polymers and give results comparable with literature data, in general obtained by 10-20 °C/min heating rates [37]. To prevent the degradation differences determined by pan and gas types, platinum pans and nitrogen gas, respectively, were used [38,40-42]. Moreover, to avoid the uncertainty from the manually determination of the T_{onset} tangent point, we considered T_{onset} the temperature at 5% weight loss, as previously reported [41]. TGA values reported in Tables. 1, 2 are average of triplicate measurements of each sample with a standard deviation ± 1-1.5 °C.

ILs TGA data (Table 1) show that HdmimDMSIP is stable up to 340 °C, whereas $OOMmimPF_6$ is stable up to 240 °C. Degradation of both ILs occurs in a single step, recording the maximum degradation temperature at 411 °C for HdmimDMSIP and at 271 °C for $OOMmimPF_6$. Moreover, it was registered a higher residue (~16%) from degradation of HdmimDMSIP with respect to that of $OOMmimPF_6$ (~9%).

Table 1. Thermal degradation of the ILs HdmimDMSIP and $OOMmimPF_6$

Samples	$T_{\Delta m}= 5\%$ (°C)[a]	Td(°C)[b]	%R[c]
HdmimDMSIP	340	411	16

OOMmimPF$_6$	240	271	9

As stated in literature data [43,44], decomposition temperatures are mainly due to the anion coordinating nature, whereas the nature of the cation, with regards to alkyl chain length, shows a weak effect. In particular, thermal stability of the highly coordinating halide anions (Cl, Br) is much lower than that of poor coordinating anions as PF$_6$. Nevertheless, reduction of thermal stability was also observed with the introduction of alkoxylated side chains in imidazolium, pyrrolidinium and piperidinium cations [42]. The presence of an alkoxylated side chain in the cation of the OOMmimPF$_6$ IL affected its thermal stability even it is constituted by the weak coordinated PF$_6^-$ anion, confirming the influence of the cation on ILs thermal stability.

In Table 2 the thermal degradation values of neat PVC and PVC/ILs compounds are reported. Neat PVC shows two thermal degradation steps (Figs. SI 10, SI 11). The first step, starting at about 200 °C, is due to hydrochloric acid loss (~60% w/w), whereas during the second one (starting at about 360 °C) degradation of new formed polyenic chains occurs [45].

Table 2 Thermal degradation of neat PVC, PVC/HdmimDMSIP and PVC/OOMmimPF6 blends

Samples	$T_{\Delta m=5\%}$ (°C) [a]	T_{d1} (°C) [b]	T_{d2} (°C) [c]	% R [d]
Neat PVC	264	313	461	9
PVC/0.1% HdmimDMSIP	256	297	466	9
PVC/0.5% HdmimDMSIP	241	285	467	9
PVC/1% HdmimDMSIP	244	282	464	9
PVC/5% HdmimDMSIP	232	251	465	10
PVC/10% HdmimDMSIP	228	246	464	10
PVC/0.1% OOMmimPF$_6$	262	307	461	7
PVC/0.5% OOMmimPF$_6$	257	302	459	5
PVC/1% OOMmimPF$_6$	258	295	461	5
PVC/5% OOMmimPF$_6$	253	293	463	6
PVC/10% OOMmimPF$_6$	251	288	461	9

In general, at temperature below 200 °C, no significant differences between neat PVC and PVC/ILs blends were found, whereas at temperatures higher than 200 °C almost all the samples of both PVC/ILs blends showed a decreasing trend of the onset temperature with increasing percentage of ILs into polymer matrix. The same trend was observed for the temperatures of the first step of degradation (T_{d1}). The second step of thermal degradation (T_{d2}) showed only slight variations (up to 6 °C) between neat PVC and PVC/ILs blends.

Considering the T_{d1}, we found a significant decrease of temperature (up to 67 °C) with increasing percentage of HdmimDMSIP. The lower thermal stability of PVC/ILs samples could be due to the IL taking part in the catalytic degradation of PVC, similar to the above mentioned autocatalytic degradation of PVC by HCl loss as PVC degrades [24]. As previously reported [26], the shift to slightly lower temperatures is probably due to the capability of ILs to anticipate or postpone dehydrochlorination of chlorine atoms from PVC chains. In a study regarding the preparation of PVC/IL blends by melt extrusion, Choi et al. [28] also suggested that the difference in thermal stability could be due to the different ILs solvating power with respect to traditional plasticizers such as DOP, with the consequence that solvated parts of PVC undergo decomposition at lower temperatures. A similar lowering of thermal decomposition induced by the introduction of ILs into polymer matrix was observed in other polymer materials. Rogalsky et al. [29] found that PC/IL compounds had reduced decomposition temperature in comparison with the neat PC. They reported that pure PC shows a single step degradation with maximum weight loss rate at 501 °C, whereas PC/IL compounds display a two-step degradation process. They suggested that the first decomposition step (at about 300-350 °C) implies the initial thermal degradation of IL products. Nevertheless, the introduction of ILs into polymer matrices do not always determine lowering of thermal decomposition. Indeed, Guo et al. [27] reported that copolymerization with ILs improved the thermal stability of PET material, founding that the introduction of ILs enhanced thermolysis temperature of PET–IL with respect to that of neat PET. In a study regarding the preparation of imidazolium PBT ionomers with ionic group located randomly along the polymer chain or selectively as end-group (telecheric), Colonna et al. [20] found that thermal stability of ionomers was similar to PBT, slightly decreasing (up to a maximum of 8 °C) with IL content.

The residue of PVC/OOMmimPF$_6$ blends, observed at 600 °C, decreased from 9% of neat PVC to 5%, proportionally to the amounts (0.1–5%, w/w) of IL loaded into blends, whereas it is similar to

that of neat PVC for IL highest concentration (10%, w/w). In the case of PVC/HdmimDMSIP blends containing low concentrations (0.1-1%, w/w) of IL the residue is not different with respect to that of neat PVC. For higher IL concentrations (5-10%, w/w) it was observed a slight increase in the residue, probably due to the involvement of ILs in the crosslinked complexes with the polyenic chains, which did not degrade up to 800 °C.

3.3. Mechanical properties

To verify the influence of ILs on the performances of PVC blends, mechanical measurements according to the microtensile ASTM D1708 were carried out. In particular, tensile strength (σ) and elongation at break (ε) were analyzed. In Figs. 3, 4 the mechanical properties of PVC containing 0.1-10% w/w of ILs are reported.

The analysis of the mechanical properties of samples demonstrated that the presence of ILs into PVC formulation slightly influence their mechanical behavior, inducing a slight plasticizing effect.
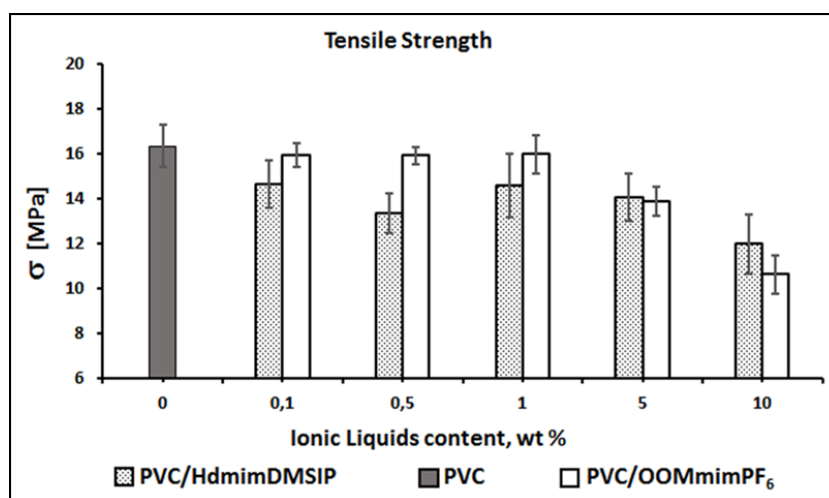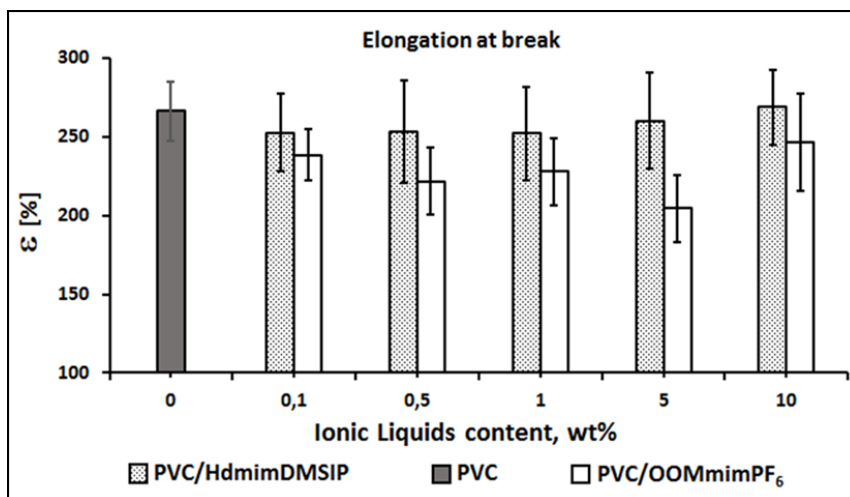

Fig. 3. Tensile strength of neat PVC, PVC/HdmimDMSIP and PVC/OOMmimPF$_6$ blends as a function of ILs content. Y-error bars standard deviation.

A slight decrease of tensile strength values and no remarkable variations of elongation at break with respect to neat PVC were registered for PVC/HdmimDMSIP blends, whereas the addition of OOMmimPF$_6$ into PVC matrix slightly decreases both tensile strength, only at higher percentages (5-10%), and elongation at break, at all percentages (Figs. 3, 4).

Our results are in agreement with literature data. Hou and Wang [25] reported that PVC resin plasticized with ILs showed tensile strength and elastic modulus decreased, while the elongation at break was enhanced. Considering the lowering of elastic modulus, they speculated that increase of flexible side-chain length indicates more soft characteristics, and consequently a decrease of elastic modulus behavior. The authors suggested that ILs lubrication action weaken interface energy between PVC paste resin and plasticizer, increasing material plasticity.

Fig. 4. Elongation at break of neat PVC, PVC/HdmimDMSIP and PVC/OOMmimPF$_6$ blends as a function of ILs content. Y-error bars standard deviation

Moreover, Rahaman and Brazel [24] observed that the addition into PVC matrix of tetrabutyl ammonium dioctylsulfosuccinate [tbam$^+$][doss$^-$] induced high flexibility in terms of elongation at break, whereas the loading of hexylmethylimidazolium dioctylsulfosuccinate [hmim$^+$][doss$^-$] showed a minor flexibility effect. They ascribed this different lubricating behavior to cation contribution as both ILs had the same anion. Indeed, the [tbam$^+$] cation showed a relatively coordinating charge surrounding four alkyl chains, whereas the [hmim$^+$] displayed high solvating effect. In the case of ILs with dodecylbenzenesulfonate [dbs] and methanesulfonate [mes] anions, they found that replacement of butyl groups by hexyl groups in the phosphonium cations, made ILs more lubricating, with consequent decrease of elastic modulus and increase of elongation at break.

3.4. SEM

The morphologies of the PVC/ILs films, detected by SEM, are showed in Fig. 5. As it can be seen from the images, the ILs introduction into PVC matrix plays an important role on surface morphology of PVC/ILs blend films.

While neat PVC (Fig. 5A) did not show any peculiar feature, PVC blends loaded with 5%-10% of ILs (Figs. 5C, 5D, 5F, 5G) displayed morphological modifications, resulting in irregular and rough surfaces. In particular, the blends containing 1% of both ILs (Figs. 5B, 5E) did not present significant modifications of sample morphology, exhibiting only a slight increase in surface roughness. Moreover, the PVC/5%-10% HdmimDMSIP blend films (Figs. 5C, 5D) displayed an oriented and more compact morphology compared with that of PVC/5%-10% OOMmimPF$_6$ (Figs. 5F, 5G), showing irregular like-island structures [31] and several cracks on film surface. It was previously reported [30] that the addition of C$_{16}$MImCl and C$_{16}$MImMeS into PLA matrix induced different surface morphologies (spheres or lines) due to PLA-ILs interaction. The size of surface spheres decreased with increasing ILs concentration. High ILs concentrations (5-10%) caused a further reduction of spheres size, until their disappearance, and appearance of a directional orientation, with formation of lines on the surface films.
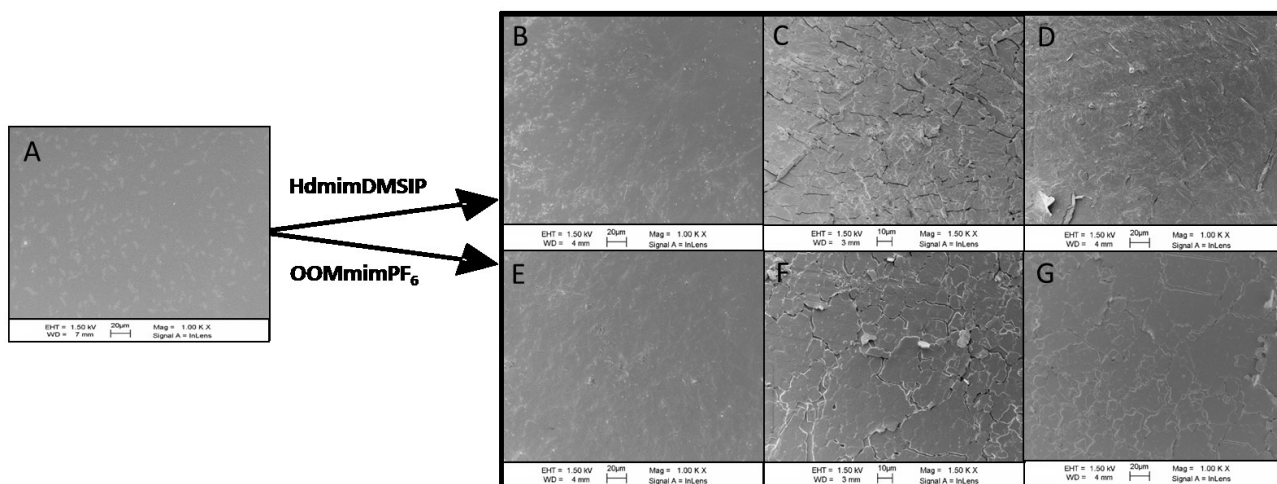

Fig. 5. SEM pictures of **A** neat PVC, **B**, **C**, **D** PVC/ HdmimDMSIP (1%, 5%, 10%) and **E**, **F**, **G** PVC/ OOMmimPF$_6$ (1%, 5%, 10%) blend films.

These results indicate that 5-10% ILs concentrations are excessive to obtain homogenous surface films, suggesting ILs surface segregation. Moreover, the ILs aggregation observed on the polymer surface increased with increasing ILs concentration, as previously reported [29, 31].

3.5. Contact Angle

Wettability of neat PVC and PVC/ILs films was characterized by measuring water drop contact angle. The effect of different weight percent of ILs (1%, 5%, 10%) on the contact angles of PVC blends was investigated. The unloaded PVC (Fig. 6) is a hydrophobic material (93.2°), whereas PVC blend films loaded with both ILs are hydrophilic.

Among factors that can influence contact angle measurements, surface texture (roughness, particles shape and size) plays an important role. Indeed, increasing surface roughness the CA decreases for neat hydrophilic materials and increases for neat hydrophobic ones [46]. Moreover, IL structure and chemical composition influence blends wettability. As previously observed [43], the cation hydrophobicity increases with the increase of alkyl chain length, whereas hydrophilicity/hydrophobicity of anions depends on their coordination ability (H-bonding capability). Furthermore, Deng et al. [47] reported that the octanol-water partition coefficient decreases with the introduction of ether and ester groups in the alkyl side chain of cation, with consequent reduction of IL lipophilicity.

In our study, the PVC blends were loaded with ILs constituted of different anions and cations. The addition of high concentrations (5%-10%) of both ILs to PVC matrix made their corresponding surface blends rough, as observed by SEM analysis. Nevertheless, their addition induced a different reduction of CA with respect to neat polymer, suggesting a higher contribution of ILs nature than surface roughness, as previously observed [31]. In particular, when the HdmimDMSIP concentration increased up to 10%, the contact angle values of the treated PVC films decreased from 93.2° to 34.28°, while the loading of OOMmimPF$_6$ in the PVC matrix induced a minor decrease of CA values from 93.2° to 76.3° (Fig. 6). In the blends loaded with the same IL, the concentration is decisive for surface morphology, with the higher IL concentrations (5-10%) that determine surface roughness. According to their content both ILs confer roughness to PVC surface, nevertheless, the same concentrations of the different ILs determine different values of contact angle, suggesting a higher hydrophilic effect of HDmimDMSIP than that of OOMmimPF$_6$. The very similar CA values of the PVC films loaded with 5%-10% of both ILs are supported by SEM images (Figs. 3C, 3D, 3F, 3G), showing surface morphologies similar for the PVC/5-10% ILs blends containing the same IL.

The HdmimDMSIP consists of a cation with a long alkyl chain, which makes it more hydrophobic, and the DMSIP anion less hydrophobic than PF$_6$. The reduced CA values of its corresponding PVC blends confirm the anion contribution to polymer wettability, as previously ascertained [27]. A specific orientation of the hydrophobic hexadecyl side chain toward the PVC matrix and the hydrophilic imidazolium ring and anion toward the polymer surface could occur, thus making PVC

blend surface hydrophilic, as previously observed in PLA loaded with different concentration of ILs bearing long alkyl chains (C_{16}MImCl and C_{16}MImeS) [30].
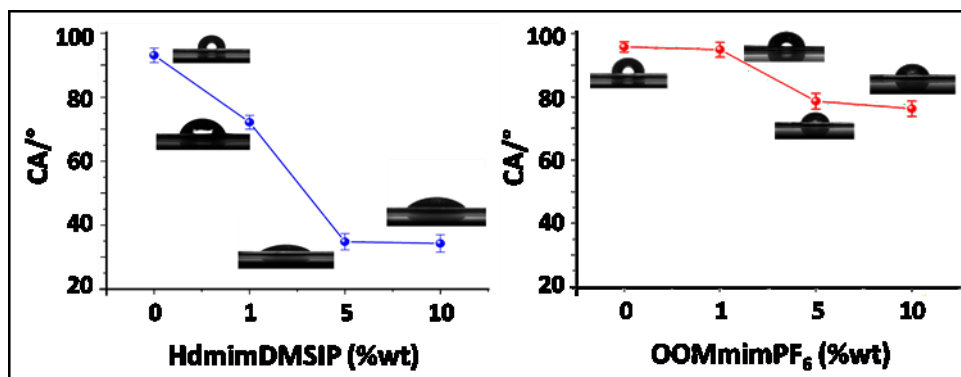

Fig. 6. Water contact angle of PVC blends as function of HdmimDMSIP and OOMmimPF$_6$ weight percent

In the case of OOMmimPF$_6$, the minor hydrophobicity of the short alkoxymethyl chain seems counterbalanced by the higher hydrophobicity of the anion, thus inducing only a small CA decrease for its corresponding PVC blends.

These results confirm that wettability of polymers can be easily tuned for specific applications by the addition of suitable ILs. In this study, HdmimDMSIP makes PVC blend surface hydrophilic, an attractive polymer property to prevent bacterial adhesion and therefore to avoid the formation of bacterial biofilms, responsible for antibiotic resistance.

3.6. ILs release

The concentration of cations and anions released from PVC/ILs blends in distilled water after the fixed incubation times was calculated by the construction of the related calibration curves (Fig. SI 12). The total amount (µg/mL) of ILs released after 1, 5, 10 and 15 days of incubation showed a linear increase during the examined period (Fig. 7), indicating that a continuous release of ILs from PVC blends occurred during the examined period. In addition, the marked release of the OOMmim from PVC/10% OOMmimPF$_6$ blend suggests the minor compatibility of this cation with PVC matrix.
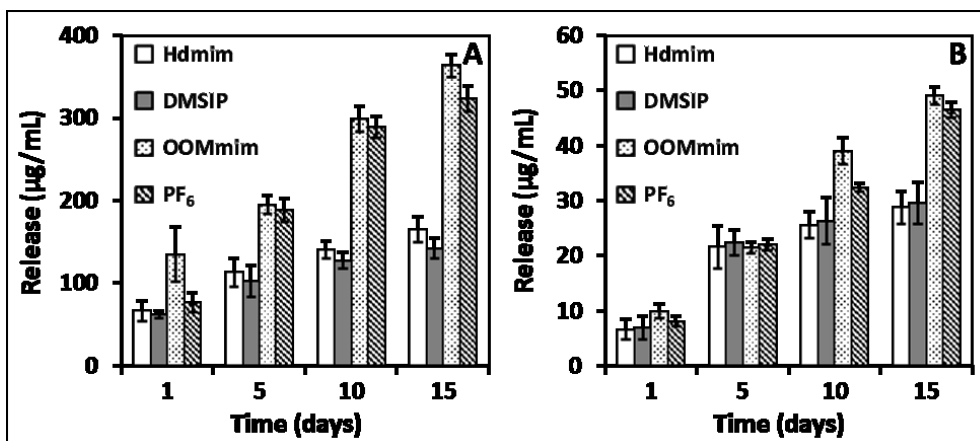
Fig. 7. Total amount of ions released in 1, 5, 10, 15 days from films of (A) PVC/10% ILs (w/w) and (B) PVC/1% ILs (w/w) in sterile water as a function of time. Y-error bars standard deviation.

To take more information on ILs release behavior over time, during the same period of observation (10 days) the daily release of ILs from PVC blends was carried out. As can be seen in Figs. SI 13, SI 14, the amount of the OOMmim cation released from PVC/10% OOMmimPF$_6$ blend is always much higher than that of the Hdmim. Moreover, the ILs release from PVC/10%ILs blends highlights values one order of magnitude higher than those from the parent PVC/1% ILs samples, confirming that ILs release is dose-dependent.

As observed by SEM analysis, the 5%-10% ILs concentrations are excessive and therefore not suitable for addition into PVC matrix because causes ILs aggregation on polymer surface and consequently their fast and quick release. We observed a less compatibility between PVC and OOMmimPF$_6$ with respect to that between PVC and HdmimDMSIP, highlighted by the higher release, mainly during the first 24 hours, of OOMmimPF$_6$ ions. In general, polymer to ILs ratio and ILs solubility in the surrounding environment are important factors for the retention of ILs into polymer matrix [48]. To this regards, the OOMmim, being more hydrophilic, was released at the highest amount during the first day of PVC/ILs membrane immersion in water, whereas the counter-ion PF$_6$, due to its lipophylicity, was released in an amount about half of the corresponding cation. In the case of PVC/HdmimDMSIP blends, the steric hindrance of both cation and anion and their higher compatibility with the polymer matrix determined a minor release, as previously reported for PC loaded with ILs bearing longer alkyl chains [29].

Data of the first day showed a release of HdmimDMSIP and OOMmimPF$_6$ from their corresponding PVC/10% ILs blends of 6.4% and 10.6%, respectively (Fig. 8). The release from PVC/1% ILs blends was 6.8% (HdmimDMSIP) and 8.4% (OOMmimPF$_6$).

These release values are less than those found adding the same ILs into Pebax®Rnew matrix [31], confirming that ILs composition, compatibility with polymer matrix and solubility in the surrounding environment are key factors for polymer/ILs membranes stability [48].
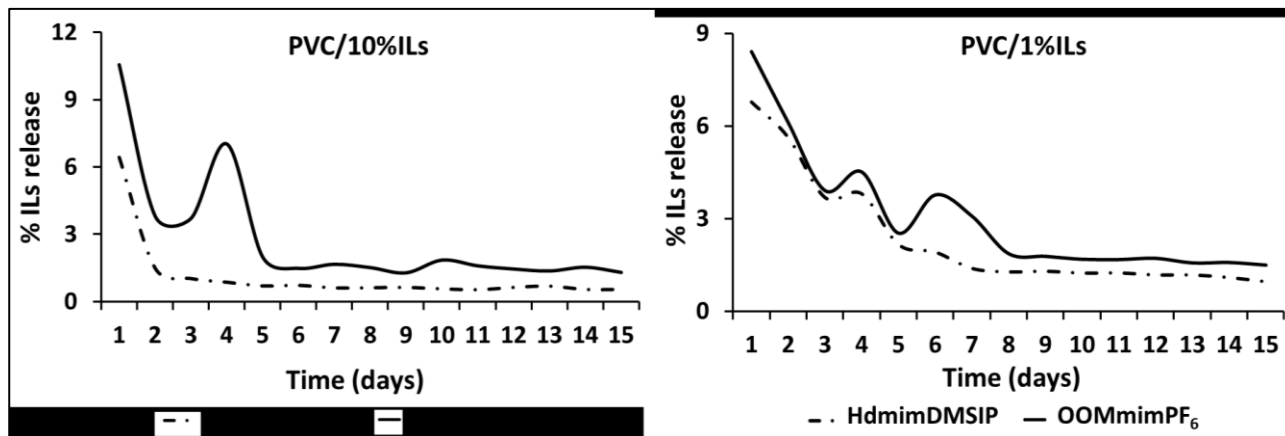

Fig. 8. Percentages of HdmimDMSIP and $OOMmimPF_6$ released in sterile water as a function of time from PVC/10% ILs (w/w) and PVC/1% ILs (w/w) blends.

Moreover, we noticed a different release behavior. The $OOMmimPF_6$ release from PVC/10% $OOMmimPF_6$ was not constant, showing, after its maximum in the first day, due to IL placed on polymer surface, another maximum in the 4th day, most probably due to the delayed migration in the polymer surface of IL trapped in the polymer matrix. On the contrary, the HdmimDMSIP release was more regular, showing after the first days a continuous decreasing release that became almost steady from the 5th day on. The release behavior from PVC/1% ILs blends was similar for both ILs. After the maximum in the first day, it displayed other two maxima in the 4th and 6th days, less pronounced for HdmimDMSIP.

Similar trends were previously observed [23, 24]. Indeed, studying the effect of the immersed time and environment media on migration from 20 wt% [bmim]PF_6 or [hmim]PF_6 plasticized PVC samples, Hou and Wang [24] reported that plasticizers could be detected after 1 day in water environment, due to the relatively weaker interaction between plasticizers and PVC paste resin. After the first day, the migration sped up gradually due to diffusion process. The partial diffusion of the plasticizer molecules into environment media produced empty holes that increased contact area of solvent molecules and membrane samples, finally accelerating exchange rate.

Rahaman and Brazel [23] reported that most of the weight loss in water from PVC samples containing 20 wt% plasticizers takes place on the first day and stabilizes after a week. They assumed that the water small molecules can easily diffuse through the wide enough pores of polymer membranes,

reaching and solubilizing the plasticizer molecules. Once the plasticizers in the outer layers are removed, leaching will depend on the strength of the existing secondary bonding effect in the polymer-plasticizer system and miscibility of the respective plasticizers with water.

3.7.   Antibacterial properties

The antibacterial activity of the neat ILs was tested in triplicate by the broth dilution method. The IL HdmimDMSIP showed both MIC and MBC values against *S. epidermidis* growth of 10 µg/mL, whereas OOMmimPF$_6$ displayed values of 3.12 µg/mL and 12.5 µg/mL, respectively. Both ILs showed MIC and MBC values vs *E. coli* of 100 and 500 µg/mL, respectively. The MBC values against *S. epidermidis* growth for both ILs are similar, whereas the MIC value for the neat OOMmimPF$_6$ was higher than that of HdmimDMSIP. This is probably due to many factors, as introduction of ether group into alkyl chain of OOMmimPF$_6$, poor coordinating nature of its anion, less steric hindrance, etc, that could improves antimicrobial effect of OOMmimPF$_6$, facilitating its diffusion into bacteria cell wall. MIC and MBC data suggest a higher sensitivity of *S. epidermidis* than that of *E. coli,* as previously observed [21,49-52]. Nevertheless, Demberelnyamba et al. [3], analyzing antibacterial activity of different ILs with long alkyl chains (C$_{12}$-C$_{16}$), found MIC values very similar for both Gram+ and Gram- bacteria.

The direct inhibition of bacteria growth induced by the PVC/ILs blend films was evaluated using the agar diffusion method. In Table 3 the diameters (mm) of the inhibition zones induced by PVC samples loaded with increasing concentrations of both ILs and neat PVC, for comparison, on TSA spread with both strains, are reported.

PVC samples containing 0.1-10% (w/w) of both ILs showed antimicrobial activity, testified by the formation of well-defined areas without growth of bacteria around the samples (Fig. SI 15). The inhibition zones induced by PVC blends on TSA plates spread with *E. coli* ranged from 1.0 (PVC/1% HdmimDMSIP) to 3.0 mm (PVC/10% HdmimDMSIP). PVC/HdmimDMSIP films displayed a higher antimicrobial activity towards the growth of *S. epidermidis* and exhibited inhibition zones ranging from 1.0 (PVC/0.1% HdmimDMSIP) to 15.3 mm (PVC/10% HdmimDMSIP). The analysis of the antibacterial activity of PVC blends loaded with different percentages of OOMmimPF$_6$ allowed to detect inhibition zones against the growth of *E. coli* ranging from 0.5 (PVC/0.5% OOMmimPF$_6$) to 5.8 mm (PVC/10% OOMmimPF$_6$). The inhibition haloes against *S. epidermidis* growth ranged from 6.8 (PVC/0.1% OOMmimPF$_6$ to 11.0 mm (PVC/10% OOMmimPF$_6$) (Table 3).

Results on inhibition haloes induced by PVC/ILs blends confirm that their antimicrobial activity is dose-dependent. Nevertheless, the width of the haloes is very similar for the higher concentrations

(1-10%) of PVC/OOMmimPF$_6$, whereas the PVC/HdmimDMSIP blends induced more regular decreasing haloes, in accordance with the IL concentration added. This different behavior suggests a greater diffusion in agar of OOMmimPF$_6$ than HdmimDMSIP, probably due to its smaller size and steric hindrance and also to the presence of an oxygen atom in the cation side alkyl chain which makes OOMmim more polar and less hydrophobic than Hdmim. This trend was confirmed by ILs release results.

The antimicrobial activity of the investigated blends was distinctly higher for the Gram-positive bacterium than the Gram-negative one, as previously observed in PBT [20]. On the contrary, this behavior was not observed in a previous study on Pebax®Rnew/ILs blends [27]. Indeed, analyzing the antimicrobial activity of Pebax®Rnew blends containing the same ILs against the growth of other Gram+ (*Listeria monocytogenes* and *Bacillus subtilis*) and Gram- (*Pseudomonas fluorescens*, *Salmonella enterica* and a different strain of *E. coli*) bacteria, we obtained results of inhibition halos different from those of the present study. Considering these findings, the antimicrobial activity of the ILs studied seems to be related not only to the wall structure but also to other physiological characteristics of the single strain analyzed [50]. Furthermore, PVC/OOMmimPF$_6$ blends at all IL concentrations showed antibacterial activity against *E. coli* higher than that of PVC/HdmimDMSIP blends. This can be explained by the higher release from PVC blends and diffusion on agar of OOMmimPF$_6$, suggesting its minor compatibility with the polymer.

Table 3. Inhibition haloes (mm, average of three replicates) induced by PVC loaded with increasing concentrations of HdmimDMSIP and OOMmimPF$_6$ and neat PVC, for comparison, on TSA plates seeded with inocula of *E. coli* and *S. epidermidis* at an initial concentration of 10^6 CFU/mL and incubated for 24 h. NI no inhibition

Samples	*S. epidermidis* Average* (mm) ± SD	*E. coli* Average* (mm) ± SD
Neat PVC	NI	NI
PVC/0.1% HdmimDMSIP	1.0 ± 0.1	NI
PVC/0.5% HdmimDMSIP	4.0 ± 0.1	NI
PVC/1% HdmimDMSIP	8.0 ± 0.1	1.0 ± 0.2
PVC/5% HdmimDMSIP	9.5 ± 2.1	2.0 ± 0.5
PVC/10% HdmimDMSIP	15.3 ± 3.1	3.0 ± 0.9
PVC/0.1% OOMmimPF$_6$	6.8 ± 1.8	NI

PVC/0.5% OOMmimPF$_6$	8.8 ± 0.6	0.5 ± 0.0
PVC/1% OOMmimPF$_6$	10.2 ± 1.4	2.2 ± 0.5
PVC/5% OOMmimPF$_6$	10.8 ± 0.3	3.3 ± 0.3
PVC/10% OOMmimPF$_6$	11.0 ± 1.0	5.8 ± 1.2

* Average of three replicates

As previously reported [3,4], the antimicrobial activity of imidazolium based ILs is due to electrostatic interactions between ILs cations and phosphate groups on the microbial cell wall. It increases with the length increase of the cation alkyl chain. Moreover, the introduction of ether-hydroxyl groups into alkyl chain enhances the antimicrobial activity with respect of that of the corresponding alkylated ILs [48,49]. Our results on MICs for neat ILs are in good agreement with data reported for antimicrobial activity of other imidazolium-based ILs [3,4,21,49]. Nevertheless, differences in MICs values could be mainly due to the different strain tested and the different methods used to execute antimicrobial susceptibility tests [52]. Considering the antimicrobial activity of PVC/ILs blends, the less hydrophobicity and the minor steric hindrance of OOMmimPF$_6$ enhances its release and consequently its antimicrobial effect, as previously observed [29]. Indeed, PC/ILs films displayed high activity against the *E. coli* bacterium, with an evident dose-dependence on IL content and no effect of cation alkyl chain length. The authors hypothesized that the more active IL bearing longer alkyl chain, being more hydrophobic, is released at a lower rate from the PC film than IL with shorter alkyl chains.

3.8.   Cytotoxicity tests

Data from the direct cytotoxicity test on neat ILs are reported in Fig. 9. HdmimDMSIP showed an AB reduction percentage higher than 50% only at 1 µg/mL concentration, whereas OOMmimPF$_6$ displayed reduction percentages from 71% (1 µg/mL) to 42% (50 µg/mL) at all concentrations analyzed, confirming its higher biocompatibility.
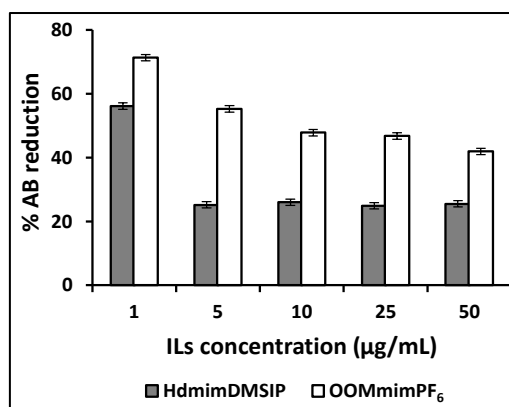
Fig. 9. Alamar blue % reduction from ILs at different concentrations

The PVC blend samples containing different amount of ILs were subjected to the indirect cytotoxicity test (elution test). To this aim the samples were first immersed in cell culture medium and then the eluates, collected at different times, were put in contact with L929 cells for 24 h and AB test was performed. The results, expressed as percentage of reduction of AB compared to the positive control, are reported in Fig. 10. It is possible to observe that percentage of AB reduction was higher for the samples with the lowest amount of HdmimDMSIP (0.1%). In particular, it was observed the 38% of the AB reduction compared to the control at the first day. This reduction increased to 45% after 5 days and reached 50% and 64% at 10 and 15 days respectively. For the samples containing higher amounts (0.5, 1, 5, 10%), AB reduction percentage was about 18-20% compared to the control at all-time points, thus suggesting that these amounts of HdmimDMSIP alter samples biocompatibility from the first day. The samples containing the lower amounts of $OOMmimPF_6$ (0.1, 0.5, 1%) showed percentages of reduction higher than 60% at 15 days. In particular, for the samples containing 0.1% the percentage of reduction is above 70%, from 76% (after 1 day) to 91% (after 15 days), at all-time points. Moreover, PVC samples containing 0.5% and 1% of $OOMmimPF_6$ exhibited AB reduction percentages of 47% and 43% (after 1 day), which increased to 75% and 78% (after 15 days), respectively. These results indicate that the loading of $OOMmimPF_6$ does not alter samples biocompatibility for percentage up to 1%. Moreover, this biocompatibility higher than that showed by PVC/HdmimDMSIP blends suggests that it can be due to the shorter alkoxymethyl chain in the imidazolium ring. Furthermore, despite its higher release than the HdmimDMSIP, the % of AB reduction in presence of all concentrations of $OOMmimPF_6$ confirms is higher biocompatibility. This is in agreement with results from the direct cytotoxicity test on neat ILs (Fig. 9) and ILs release from PVC blends (Fig. 8). Indeed, after the first day, 128.6 and 211.5 µg/mL of HdmimDMSIP and $OOMmimPF_6$, respectively, were released from the PVC/10% blends. These concentrations resulted

toxic for L929 cells as well as those observed after 5, 10 and 15 days, confirming results reported in Fig. 8. The concentration of HdmimDMSIP released after the first day from the PVC/1% blend was 13.6 µg/mL. The OOMmimPF$_6$ resulted biocompatible after 1 (17.9 µg/mL) and 5 (43.5 µg/mL) days of IL release (Figs. 7, 9). Its release concentration after 10 and 15 days was of 71.4 µg/mL and 95.6 µg/mL, respectively. These results are not in good agreements with those reported in Fig. 10, showing an increasing biocompatibility as the incubation period increases. We suppose that after 10 and 15 days saturation of the medium (2 mL volume for cytotoxicity analyses, 5 mL volume for ILs release in water), as well as IL aggregations and/or interactions with some components of the medium (proteins) could occur [52], preventing its toxicological effect. As mentioned previously, the ILs release is dose dependent, showing values from PVC/10% ILs blends one order of magnitude higher than those from PVC/1% ILs blends. A similar reduction of ILs release (one order of magnitude) could occur from PVC/0.1% ILs blends. After 1 day, concentration of ILs released from PVC/0.1% ILs blends could be ~1.3 µg/mL (HdmimDMSIP) and 1.8 µg/mL (OOMmimPF$_6$), in accordance with results shown in Figs. 9, 10, and, in particular, with the biocompatibility found for both PVC/0.1% HdmimDMSIP and PVC/0.1% OOMmimPF$_6$ blends.
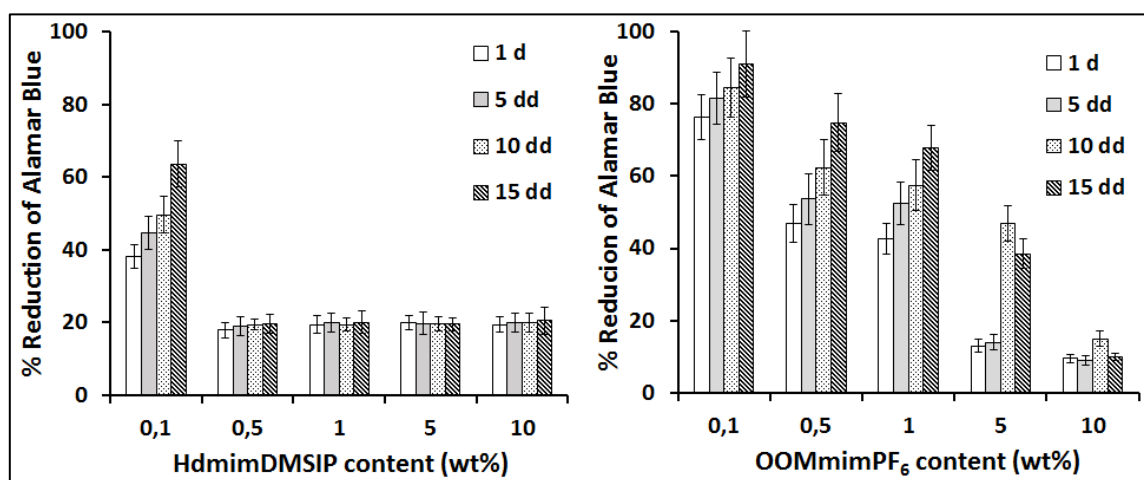

Fig. 10. Alamar blue % reduction from PVC samples loaded with different amounts of ILs

In general, ILs toxicity increases as the length of alkyl chain on cation increases. It also depends on anion contribution, being halogens (Br-Cl) less toxic than BF$_4$, PF$_6$ and NTf$_2$ [54].

Our results are in agreement with ILs toxicity analyzed by the 1-octanol/water partition coefficient. This coefficient is a toxicological parameter that evaluates substances hydrophobicity and estimates environment risk factors [55, 56]. It increases as the length of the side alkyl chain in imidazolium ILs increases, indicating higher hydrophobicity, whereas it decreases for imidazolium ILs bearing alkyl

28

chain funzionalized with ether or hydroxyl groups [47]. The OOMmimPF$_6$ is therefore less toxic than HdmimDMSIP mainly due to both short alkyl length and presence of an oxygen atom within the alkyl chain, suggesting a minor contribution of anion. Nevertheless, to this regards, the contribution of the less release of the anion with respect to that of the cation from the PVC/ OOMmimPF$_6$ blends cannot be overlooked.

4. Conclusions

In this study, two ILs were synthetized, characterized and loaded, at different amounts, as antimicrobial agents into PVC matrix. The incorporation of both ILs induced only slight modifications of the thermal and mechanical properties of PVC films, thus not influencing the processability and the formability of the material even at high IL content (10% wt). Results showed that the loading into PVC of all concentrations (0.1-10% w/w) of both ILs induced antimicrobial activity, depending on ILs concentration. Moreover, the introduction of HdmimDMSIP into PVC matrix made the polymer surface hydrophilic, a desirable anti-fouling property. The highest release amount of ILs occurred during the first day of in water incubation. Since flexible PVC formulations are widely used for biomedical applications (blood or urine bags, transfusion tubing, catheters, etc.), the realization of PVC/ILs compounds displaying antimicrobial activity represents a valuable result that could be useful for the development of PVC-based antimicrobial medical devices. In fact, the availability of antimicrobial agents on both the outer and the inner surfaces of a device is of crucial importance for medical purposes. Furthermore, both ILs at 0.1% did not have harmful effects on L929 cells and samples containing OOMmimPF$_6$ at concentrations up to 1% showed good biocompatibility as confirmed by *in vitro* tests.

Conflicts of interest

There are no conflicts to declare.

References

[1] Zampino, D.; Ferreri, T.; Puglisi, C.; Mancuso, M.; Zaccone, R.; Scaffaro R.; Bennardo, D. PVC silver zeolite composites with antimicrobial properties, J. Mater. Sci. 46 (2011) 6734–6743. https://doi.org/10.1007/s10853-011-5629y

[2] Zheng, Z.; Xu, Q.; Guo, J.; Qin, J.; Mao, H.; Wang B.; Yan, F. Structure−Antibacterial Activity Relationships of Imidazolium-Type Ionic Liquid Monomers, Poly(ionic liquids) and Poly(ionic liquid) Membranes: Eff ect of Alkyl Chain Length and Cations, Appl. Mater. Interfaces 8 (2016) 12684-12692. https://doi.org/10.1021/acsami.6b03391

[3] Demberelnyamba, D.; Kim, K.-S.; Choi, S.; Park, S.-Y.; Lee, H.; Kim, C.-J.; Yoo, Ick-Dong. Synthesis and antimicrobial properties of imidazolium and pyrrolidinonium salts, Bioorgan Med. Chem. 12 (2004) 853-857. https://doi.org/10.1016/j.bmc.2004.01.003

[4] Gilmore, B.F. Antimicrobial Ionic Liquids, in 'Ionic Liquids. Applications and Perspectives' InTechOpen (2011), Ed. A. Kokorin. https://doi.org/10.5772/13861

[5] Belay, K.; Abisa, Z. Properties, applications and synthesis of ionic liquids in Chemistry: a review, WJPMR 1 (2015) 32-39. ISSN 2455-3301

[6] Welton, T. Ionic Liquids: A Brief History, Biophys. Rev. 10 (2018) 691–706. https://doi.org/10.1007/s12551-018-0419-2

[7] Lu, J.; Yan, F.; Texter, J. Advanced applications of ionic liquids in polymer science, Prog. Polym. Sci. 34 (2009) 431-448. https://doi.org/10.1016/j.progpolymsci.2008.12.001

[8] Welton, T. Room-Temperature Ionic Liquids. Solvents for Synthesis and Catalysis, Chem. Rev. 99 (1999) 2071-2083. https://doi.org/10.1021/cr980032t

[9] Olivier-Bourbigou, H.; Magna L.; Morvan, D. Ionic Liquids and Catalysis: Recent Progress from Knowledge to Applications, Appl. Catal. A 373 (2010) 1-56. https://doi.org/10.1016/j.apcata.2009.10.008

[10] Vekariya, R. L. A review of ionic liquids: Applications towards catalytic, J. Mol. Liq. 227 (2017) 44-60. https://doi.org/10.1016/j.molliq.2016.11.123

[11] De Bon, F.; Fantin, M.; Isse A.A.; Gennaro, A. Electrochemically mediated ATRP in ionic liquids: controlled polymerization of methyl acrylate in [BMIm][OTf], Polym. Chem. 9 (2018) 646-655. https://doi.org/10.1039/C7PY02134H

[12] Wei D.; Ivaska, A. Applications of ionic liquids in electrochemical sensors, Anal. Chim. Acta 607 (2008) 126-135. https://doi.org/10.1016/j.aca.2007.12.011

[13] Demberelnyamba, D.; Ariunaa M.; Shim, Y.K. Synthesis of Silver Nanoparticles Using Hydroxyl Functionalized Ionic Liquids and Their Antimicrobial Activity, Int. J. Mol. Sci. 9 (2008) 807-820. https://doi.org/10.3390/ijms9050807

[14] Ye, Y.-S.; Rick J.; Hwang, B.-J. Ionic liquid polymer electrolytes, J. Mater. Chem. A 1 (2013) 2719-2743. https://doi.org/10.1039/C2TA00126H

[15] Berthod, A.; Ruiz-Ángel, M.J.; Carda-Broch, S.; Recent advances on ionic liquid uses in separation techniques, J. Chromatogr. A, 1559 (2018) 2–16. https://doi.org/10.1016/j.chroma.2017.09.044

[16] Bugatti, V.; Viscusi, G.; Di Bartolomeo, A.; Iemmo, L.; Zampino, D.C.; Vittoria, V.; Gorrasi, G. Ionic Liquid as Dispersing Agent of LDH-Carbon Nanotubes into a Biodegradable Vinyl Alcohol Polymer, Polymers 12 (2020) 495. https://doi.org/10.3390/polym12020495

[17] Bernardo, P.; Zampino D.; Clarizia, G.; Triggering the gas transport in PVdF-HFP membranes via imidazolium ionic liquids, Sep. Purif. Technol. 250 (2020) 117201. https://doi.org/10.1016/j.seppur.2020.117201

[18] Ferraz, R.; Branco, L.C.; Prudêncio, C.; Noronha J.P.; Petrovski, Ž. Ionic Liquids as Active Pharmaceutical Ingredients, ChemMedChem, 6 (2011) 975 – 985. https://doi.org/10.1002/cmdc.201100082

[19] Anderson, E. B.; Long, T. E. Imidazole- and imidazolium-containing polymers for biology and material science applications, Polymer 51 (2010) 2447-2454. https://doi.org/10.1016/j.polymer.2010.02.006

[20] Colonna, M.; Berti, C.; Binassi, E.; Fiorini, M.; Sullalti, S.; Acquasanta, F.; Vannini, M.; Di Gioia, D.; Aloisio, I. Imidazolium poly(butylene terephthalate) ionomers with long-term antimicrobial activity, Polymer 53 (2012) 1823–1830. https://doi.org/10.1016/j.polymer.2012.03.003

[21] Łuczak, J.; Jungnickel, C.; Łacka, I.; Stolte S.; Hupkaa, J. Antimicrobial and surface activity of 1-alkyl-3-methylimidazolium derivatives, Green Chem. 12 (2010) 593-601. https://doi.org/10.1039/B921805J

[22] Pendleton, N.; Gilmore, B. F. The antimicrobial potential of ionic liquids: A source of chemical diversity for infection and biofilm control, Int. J. Antimicrob. Agents 46 (2015) 131–139. https://doi.org/10.1016/j.ijantimicag.2015.02.016

[23] Scott, M. P.; Rahman M.; Brazel, C. S. Application of ionic liquids as low-volatility plasticizers for PMMA, Eur. Polym. J. 39 (2003) 1947-1953. https://doi.org/10.1016/S0014-3057(03)00129-0

[24] Rahman, M.; Brazel, C. S.; Ionic liquids: New generation stable plasticizers for poly(vinyl chloride), Polym. Degrad. Stab. 91 (2006) 3371-3382. https://doi.org/10.1016/j.polymdegradstab.2006.05.012

[25] Hou, L. X.; Wang, S. Study on ionic liquid [bmim]PF6 and [hmim]PF6 as plasticizer for PVC paste resin., Polym. Bull. 67 (2011) 1273-1283. https://doi.org/10.1007/s00289-011-0490-3

[26] Choi, S. Y.; Rodrìguez, H.; Mirjafari, A.; Gilpin, D. F.; McGrath, S.; Malcolm, K. R.;. Tunney, M. M; Rogers R. D.; McNally, T. Dual functional ionic liquids as plasticisers and antimicrobial agents for medical polymers, Green Chem. 13 (2011) 1527. https://doi.org/10.1039/C1GC15132K

[27] Guo, N.; Hu, D.; Wang, H.; Wang R.; Xiong, Y. Functional poly (ethylene terephthalate) materials prepared by condensation copolymerization with ionic liquids, Polym. Bull. 70 (2013) 3031–3040. https://doi.org/10.1007/s00289-013-1005-1

[28] Choi, Y.; Rodrìguez, H.; Gunaratne, H. Q. N.; Puga, A. V.; Gilpin, D.; McGrath, S.; Vyle, J. S.; Tunney, M. M.; Rogers R. D.; McNally, T. Dual functional ionic liquids as antimicrobials and plasticisers for medical grade PVCs., RSC Adv. 4 (2014) 8567-8581. https://doi.org/10.1039/C3RA46425C

[29] Rogalsky, S.; Fatyeyeva, K.; Lyoshina, L.; Tarasyuk, O.; Bulko, O.; Lobok, S. Antimicrobial Properties and Thermal Stability of Polycarbonate Modified with 1-Alkyl-3-methylimidazolium Tetrafluoroborate Ionic Liquids, J. Appl. Polym. Sci. (2014) 40050–40056. https://doi.org/10.1002/app.40050

[30] Schrekker, C. M. L.; Sokolovicz, Y. C. A.; Raucci, M. G.; Selukar, B. S.; Klitzke, J. S.; Lopes, W.; Leal, C. A. M.; De Souza, I. O. P.; Galland, G. B.; Dos Santos, J. H. Z.; Mauler, R. S.; Kol, M.; Dagorne, S.; Ambrosio, L.; Teixeira, M. L.; Morais, J.; Landers, R.; Fuentefria A. M.; Schrekker, H. S. Multitask Imidazolium Salt Additives for Innovative Poly(l-lactide) Biomaterials: Morphology Control, Candida spp. Biofilm Inhibition, Human Mesenchymal Stem Cell Biocompatibility, and Skin Tolerance, ACS Appl. Mater. Interfaces, 8, (2016) 21163-21176. https://doi.org/10.1021/acsami.6b06005

[31] Clarizia, G.; Bernardo, P.; Carroccio, S. C.; Ussia, M.; Restuccia, C.; Parafati, L.; Calarco A.; Zampino, D. Heterogenized Imidazolium-Based Ionic Liquids in Pebax Rnew. Thermal, Gas Transport and Antimicrobial Properties, Polymers 12 (2020) 1419. https://doi.org/10.3390/polym12061419

[32] Raucci, M.G.; Fasolino, I.; Pastore, S.G.; Soriente, A.; Capeletti, L.B.; Dessuy, M.B.; Giannini, C.; Schrekker, H.S.; Ambrosio, L. Antimicrobial Imidazolium Ionic Liquids for the

Development of Minimal Invasive Calcium Phosphate-Based Bionanocomposites, ACS Appl. Mater. Interfaces 10 (49) (2018) 42766–42776. https://doi.org/ 10.1021/acsami.8b12696

[33] Muñoz-Bonilla, A.; Fernández-García, M. Poly(ionic liquid)s as antimicrobial materials, Eur. Polym. J. 105 (2018) 135-149. https://doi.org/10.1016/j.eurpolymj.2018.05.027

[34] Pernak, J.; Czepukowicz, A.; Pozniak, R. New Ionic Liquids and Their Antielectrostatic Properties, Ind. Eng. Chem. Res. 40 (2001) 2379–2383. https://doi.org/10.1021/ie000689g

[35] Bauer A W, Kirby W M M, Sherris J C, Turck M (1966) Antibiotic susceptibility testing by a standardized single disk method. American journal of clinical pathology 45: 493-496. https://doi.org/10.1093/ajcp/45.4_ts.493

[36] International Organization for Standardization (ISO) 10993-5, Biological evaluation of medical devices Part 5: Tests for in vitro cytotoxicity, 2009. https://www.iso.org/standard/36406.html

[37] Bonhôte, P.; Dias, A.-P.; Papageorgiou, N.; Kalyanasundaram K.; Grätzel, M. , Hydrophobic, Highly Conductive Ambient-Temperature Molten Salts, Inorg. Chem., 35 (1996) 1168-1178. https://doi.org/ 10.1021/ic951325x

[38] Fradelake, C. P.; Crosthwaite, J. M.; Hert, D. G.; Aki, S. N. V. K.; Brennecke, J. F. Thermophysical Properties of Imidazolium-Based Ionic Liquids, J. Chem. Eng. Data, 49 (2004) 954-964. https://doi.org/10.1021/je034261a

[39] Gómez, E.; Calvar N.; Domínguez, Á. in Ionic Liquids - Current State of Art, ed. Scott Handy, InTech Open Science, ISBN: 978-953-51-2122-0, 2015, 8, 199-228. http://dx.doi.org/10.5772/59271

[40] Ngo, H. L.; LeCompte, K.; Hargens L.; McEwen, A. B. Thermal properties of imidazolium ionic liquids, Thermochim. Acta 357-358 (2000) 97-102. https://doi.org/10.1016/S0040-6031(00)00373-7

[41] Awad, W. H.; Gilman, J. W.; Nyden, N.; Harris, R. H.; Sutto, T. E.; Callahan, J.; Trulove, P. C.; DeLong, H. C.; Fox, D. M. Thermal degradation studies of alkyl-imidazolium salts and their application in nanocomposites, Thermochim. Acta 409 (2004) 3–11. https://doi.org/10.1016/S0040-6031(03)00334-4

[42] Maton, C., De Vos, N.; Stevens, C. V.; Ionic liquid thermal stabilities: decomposition mechanisms and analysis tools, Chem. Soc. Rev. 42 (2013) 5963-5977. https://doi.org/10.1039/C3CS60071H

[43] Huddleston, J.G.; Visser, A.E.; Reichert, W.M.; Willauer, H.D.; Broker G.A.; Rogers, R.D.

Characterization and comparison of hydrophilic and hydrophobic room temperature ionic liquids incorporating the imidazolium cation, Green Chem. 3 (2001) 156–164. https://doi.org/10.1039/B103275P

[44] Crosthwaite, J. M.; Muldoon, M. J.; Dixon, J. K.; Anderson, J. L.; Brennecke, Phase transition and decomposition temperatures, heat capacities and viscosities of pyridinium ionic liquids, J. Chem. Thermodynamics 37 (2005) 559-568. https://doi.org/10.1016/j.jct.2005.03.013

[45] Montaudo G.; Puglisi, C., Evolution of Aromatics in the Thermal-Degradation of Poly(Vinyl Chloride) - A Mechanistic Study, Polym. Degrad. Stab., 1991, 33, 229-262. https://doi.org/10.1016/0141-3910(91)90019-N

[46] Chau, T. T.; Bruckard, W. J.; Koh, P. T. L.; Nguyen, A. V. A review of factors that affect contact angle and implications for flotation practice, Adv. Colloid Interface Sci. 150 (2009) 106–115. https://doi.org/10.1016/j.cis.2009.07.003

[47] Deng, Y.; Besse-Hoggan, P.; Saucelme, M.; Delort, A.-M.; Husson P.; Gomes, M. F. C. J. Influence of oxygen functionalities on the environmental impact of imidazolium based ionic liquids, Hazard. Mater. 198 (2011) 165-174. https://doi.org/10.1016/j.jhazmat.2011.10.024

[48] Tomàs-Alonso, F.; Rubio, A. M.; Giménez, A.; de los Rìos, A. P.; Salar-Garcìa, M. J.; Ortiz-Martìnez, V. M.; Hernàndez- Fernàndez, F. J.; Influence of ionic liquid composition on the stability of polyvinyl chloride-based ionic liquid inclusion membranes in aqueous solution, AIChE Journal 63 (2017) 770-780. https://doi.org/10.1002/aic.15460

[49] Pernak, J.; Sobaszkiewicza, K.; Mirskab, I. Anti-microbial activities of ionic liquids, Green Chem. 5 (2003) 52-56. https://doi.org/10.1039/B207543C

[50] Docherty, K.; Kulpa, C.F. Toxicity and antimicrobial activity of imidazolium and pyridinium ionic liquids, Green Chem. 7 (2005) 185–189. https://doi.org/10.1039/B419172B

[51] Garcia, M.T.; Ribosa, I.; Perez, L.; Manresa, A.; Comelles, F. Micellization and Antimicrobial Properties of Surface-Active Ionic Liquids Containing Cleavable Carbonate Linkages, Langmuir. 33 (2017) 6511-6520. doi:10.1021/acs.langmuir.7b00505

[52] Florio, W.; Becherini, S.; D'Andrea, F.; Lupetti, A.; Chiappe, C.; Guazzelli, L. Comparative evaluation of antimicrobial activity of different types of ionic liquids, Mater. Sci. Eng. C 104 (2019) 109907. https://doi.org/10.1016/j.msec.2019.109907

[53] Tang, S.; Baker G. A.; Zhao, H. Ether- and alcohol-functionalized task-specific ionic liquids: attractive properties and applications, Chem. Soc. Rev., 41, (2012) 4030–4066. https://doi.org/10.1039/C2CS15362A

[54] Frade R. F. M.; Afonso, C. A. M.; Impact of ionic liquids in environment and humans: An overview. Human and Experimental Toxicology, Hum. Exp. Toxicol. 29 (2010) 1038-1054. https://doi.org/10.1177/0960327110371259

[55] Domanska, U.; Bogel-Lukasik E; Bogel-Lukasik, R. 1-Octanol/Water Partition Coefficients of 1-Alkyl-3-methylimidazolium Chloride, Chem. Eur. J. 9 (2003) 3033–3041. https://doi.org/10.1002/chem.200204516

[56] Ventura, S. P. M.; Gardas, R. L.; Goncalves, F.; Coutinho, J. A. P. J. Ecotoxicological risk profile of ionic liquids: octanol-water distribution coefficients and toxicological data, Chem. Technol. Biotechnol. 86 (2011) 957–963. https://doi.org/10.1002/jctb.2606